Article

Single-Crystal Mesoporous ZnO Thin Films Composed of Nanowalls

Xudong Wang, Yong Ding, Zhou Li, Jinhui Song, and Zhong Lin Wang

J. Phys. Chem. C, **2009**, 113 (5), 1791-1794 • Publication Date (Web): 13 January 2009

Single-Crystal Mesoporous ZnO Thin Films Composed of Nanowalls

Xudong Wang, Yong Ding, Zhou Li, Jinhui Song, and Zhong Lin Wang*

School of Materials Science and Engineering, Georgia Institute of Technology Atlanta, Georgia 30332-0245

Received: October 22, 2008; Revised Manuscript Received: December 10, 2008

This paper presents a controlled, large scale fabrication of mesoporous ZnO thin films. The entire ZnO mesoporous film is one piece of a single crystal, while high porosity made of nanowalls is present. The growth mechanism was proposed in comparison with the growth of ZnO nanowires. The ZnO mesoporous film was successfully applied as a gas sensor. The fabrication and growth analysis of the mesoporous ZnO thin film give general guidance for the controlled growth of nanostructures. It also provides a unique structure with a superhigh surface-to-volume ratio for surface-related applications.

1. Introduction

Known as one of the most important semiconductor materials, zinc oxide (ZnO) has received intensive research interest in broad areas, including electronics, optoelectronics, and peizotronics.[1,2] Owing to its noncentrosymmetric wurtzite structure and self-polarized crystal surfaces, ZnO exhibits the most splendid family of nanostructure morphologies, such as nanobelts, nanowires (NWs), nanosprings, nanorings, nanocombs, and nanohelices.[3−7] Among them, aligned ZnO NWs with controlled size, growth direction, and surfaces have shown great potential for building nanodevices with superior mechanical, electrical, optical, and piezoelectric properties. It has been discovered that the aligned ZnO NWs sometimes came with a continuous sheet-like structure connecting the bottom of the NWs. Once the sheet became dominant, a new morphology called nanowalls appeared.[8,9] As a quasi-two-dimensional nanostructure with a high porosity, the vertically aligned ZnO nanowalls exhibit great promise for sensors, fuel cells, solar cells, and catalysts.[10] Although formation mechanisms have been proposed, lack of rational control makes the nanowall often be accompanied by aligned ZnO NWs that stand directly above, and receiving a single-phased nanowall structure becomes more or less unpredictable

In this paper, we report a controlled growth of single crystal mesoporous ZnO thin films composed of vertically aligned ZnO walls. After analyzing the growth condition and structure of the mesoporous films, we present a general understanding on the vapor concentration-induced growth orientation selection. Guided by this discovery, formation of NWs with the nanowall structure can be intentionally turned on and off so that a single-phased nanowall structure was observed repetitively. A potential application of the film as a gas sensor has also been demonstrated.

2. Experimental Section

The mesoporous ZnO film was fabricated in a double tube system. In this system, an alumina tube with 2-in. inner diameter (ID) was place inside a tube furnace with both ends sealed by a metal cap. Then a 95% Ar/5% O_2 mixture was introduced into the tube as carrying and reactive gases at a total flow rate of 50 sccm. The source materials (a mixture of 0.3 g of ZnO powder and 0.3 g of graphite power) were loaded at the center of a 20 cm long quartz tube with 0.5-in. inner diameter. The substrate used for the growth is a GaN epitaxial film grown on single crystal alumina substrate. The substrate was covered by a layer of 0.4 nm thick Au as catalyst and was placed at one end of the small tube. The small quartz tube was then positioned inside the alumina tube with both tube centers aligned together and the substrate pointing downstream of the gas flow. At a tube vacuum of 20 torr, the tube furnace was heated up to 950 °C at a rate of 50 °C /min and the substrate was located in the ∼700 °C temperature zone. The temperature and vacuum were held steady for 2 h for ZnO deposition. Then the furnace was turned off, and the tube was cooled to room temperature with the vacuum unchanged.

3. Results

The as-synthesized ZnO film exhibits white-blue color. The as-grown structure was first characterized using scanning electronic microscopy (SEM). A low-magnification SEM image reveals the high porosity surface of the ZnO film, as shown in Figure 1a. The film is rather uniform and is filled with porosity. A zoom-in image shows the sizes of pores are from 30 to 200 nm, while the ZnO walls between the pores exhibit a much more uniform thickness at ∼50 nm (inset of Figure 1a). The porous ZnO film also has a fairly uniform thickness across the entire substrate. As shown by a cross-section SEM image (Figure 1b), the overall film thickness is ∼2 μm. However, small variations (mostly between ± 10 nm) can be observed because of the nonflat top of the ZnO walls. All of the pores, regardless of their size, are straight and extend all the way through the film to the supporting substrate. This feature is clearly displayed by a higher magnification SEM image of the cross-section sample (Figure 1c). Significantly, the growth position of the porous film can be precisely controlled by patterning the Au catalyst film, similar to the patterned growth of NWs. As shown in Figure 1d, ZnO porous film only grew on the Au covered area, and a very sharp edge is presented at the Au−no Au boundary.

Unlike most other porous structures, the entire piece of the ZnO mesoporous film is a single crystal. An X-ray diffraction (XRD) spectrum of the as-synthesized structure only shows one strong peak at 34.8° corresponding to the (0002) atomic plane of ZnO crystal (Figure 2a). Besides, a small diffraction peak from the *a*-plane alumina substrate was also observed. The diffraction peak of GaN buffer layer was completely overlapped with the ZnO peak because of their high degree of lattice match. The XRD spectrum clearly shows the single crystal structure

* Corresponding author. E-mail: zhong.wang@mse.gatech.edu.

10.1021/jp809358m CCC: $40.75
Published on Web 01/13/2009

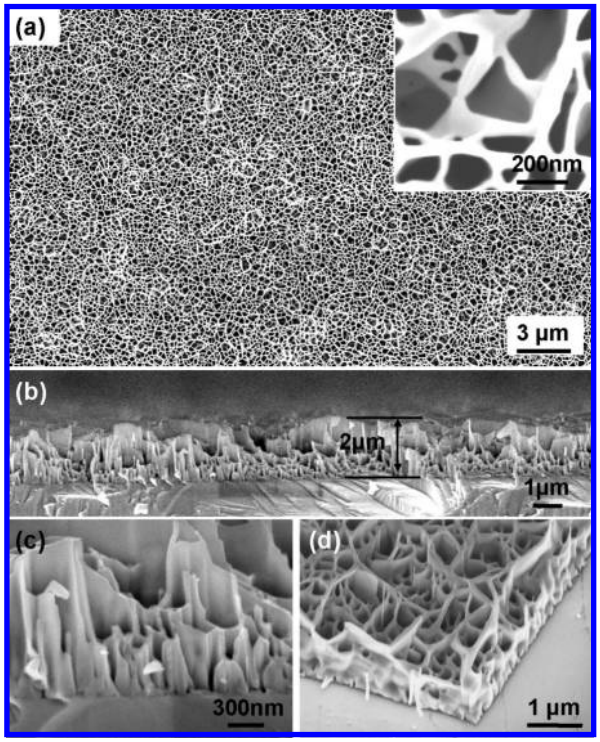

Figure 1. SEM images of ZnO mesoporous thin film on Al_2O_3 substrate with GaN buffer layer. (a) Top-view low and high magnification (inset) SEM images. (b) Cross-section image of the interface. (c and d) Side-view image of the structure.

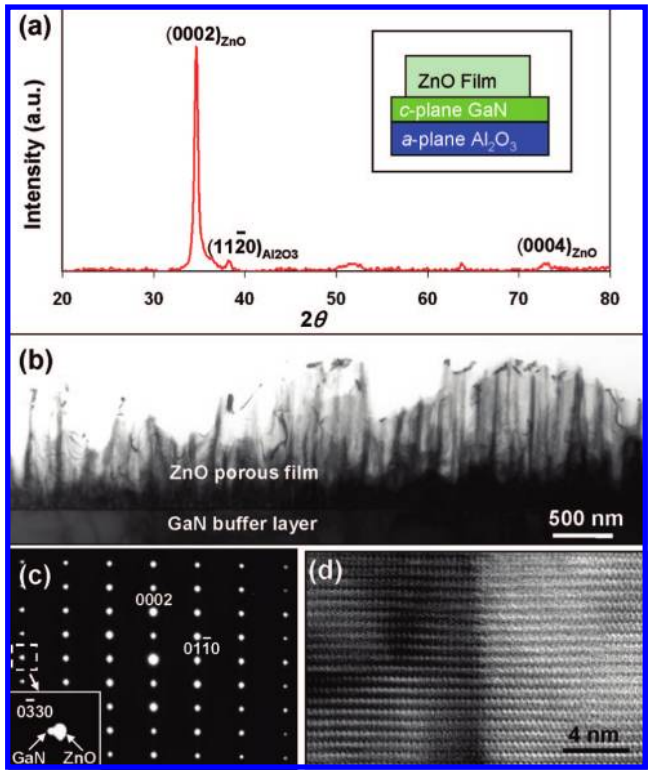

Figure 2. (a) XRD pattern of the ZnO mesoporous thin film on Al_2O_3 substrate with GaN buffer layer. The first peak around 51−52° could be ZnO (0003), and the peak located at 63.58° is from the Au (220). (b) TEM image of the GaN−ZnO interface, the select-area electron diffraction pattern is shown in c. (d) An HRTEM image of the interface between vertical and horizontal ZnO walls.

of the ZnO porous film and its epitaxial relationship with the substrate (inset of Figure 2a).

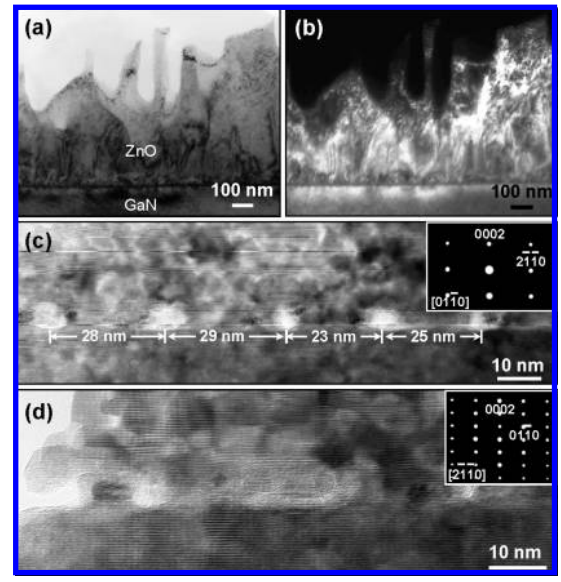

Figure 3. Bright-field (a) and dark-field (b) images of the GaN−ZnO interface to show the local strain field. (c and d) HRTEM images of the interface with the incident electron beam along the [01$\bar{1}$0] and [2$\bar{1}\bar{1}$0] direction, respectively. The diffraction conditions are inserted in each image.

The crystallography of ZnO mesoporous film was further investigated using transmission electronic microscopy (TEM). Figure 2b is a typical cross-section TEM image of the ZnO film together with the GaN buffer layer at the bottom. The orientation of the ZnO walls can be revealed by the image contrast, where the bright and dark contrasts represent walls parallel/nearly parallel or perpendicular/nearly perpendicular to the paper surface, respectively. Because of the close lattice constants of GaN and ZnO, electron diffraction taken from this cross-section sample only gives "one" set of pattern showing that the vertical and horizontal direction of both ZnO and GaN is [0002] and [01$\bar{1}$0], respectively (Figure 2c). After three periods along the ⟨01$\bar{1}$0⟩ direction, the diffraction spot of GaN can be distinguished from that of ZnO (inset of Figure 2c) owing to their difference in lattice parameters.[11,12]

A high resolution TEM (HRTEM) image was taken from the area where two pieces of ZnO walls meet, as shown in Figure 2d. The ZnO crystal lattice is continuous even across the interface between the ZnO walls pointing toward different directions. No grain boundary can be observed at the junctions. The TEM analysis confirms that the entire mesoporous film is a single-crystal ZnO epitaxially grown on the *c*-plane-oriented GaN buffer layer.

Although GaN and ZnO have close lattice constants,[11,12] strains are still induced in the grown film, as shown in Figure 3a. The distribution of such strains can be more clearly observed in Figure 3b, which is a dark-field image of the same area show in Figure 3a. Mismatch dislocations are found in the ZnO side originating from the interface. Those strains and defects could be the factor that limits the width of ZnO walls to ∼50 nm.

The HRTEM image taken at the GaN−ZnO interface revealed an interesting epitaxial relationship between ZnO and GaN. As shown in Figure 3c, a row of amorphous columns was discovered once a TEM image is taken along the [01$\bar{1}$0] zone axis. Those columns have a size of 5−8 nm and are 20−30 nm apart from each other. Formation of the columns is believed to release the lattice strain induced by lattice mismatch (Figure 3b). A small variation in intercolumn distance could be attributed to the variation in local strain around the crystal edges. It is

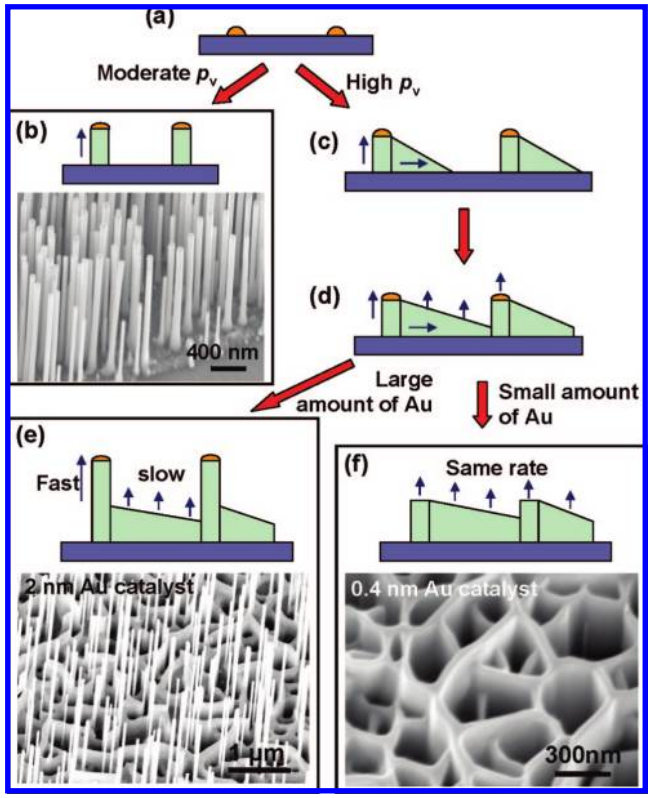

Figure 4. Growth model of the ZnO mesoporous thin film. See text for detailed description.

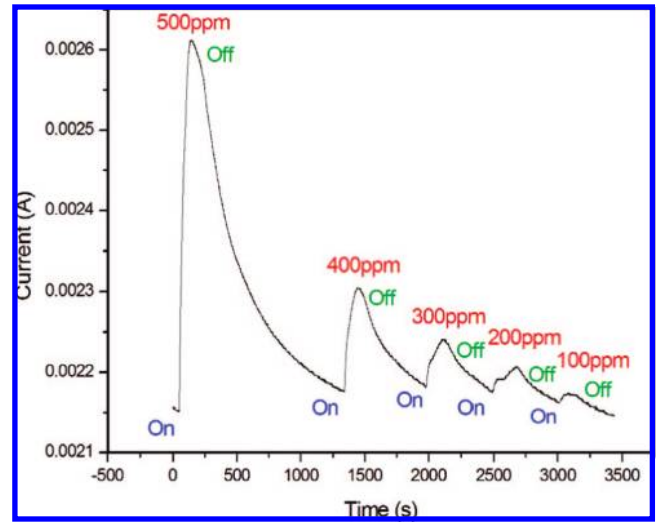

Figure 5. The response of ZnO mesoporous thin film fabricated gas sensor to CH_4 gas.

further identified that the columns only extend along the $\langle 01\bar{1}0\rangle$ direction. When the cross-section sample is tilted 30°, the columns can no longer be clearly observed in the image taken along the $[2\bar{1}\bar{1}0]$ zone axis (Figure 3(d)). Considering there are six equivalent $\langle 01\bar{1}0\rangle$ directions in the (0001) interface plane, therefore, it can be deduced that the amorphous columns are in $\langle 01\bar{1}0\rangle$ directions and form a 6-fold network at the GaN−ZnO interface. The formation of the amorphous columns can serve as indirect evidence to support the assumption that it is the interface strain that induced the formation of ZnO wall structure.

The mesoporous ZnO film was fabricated through a process very similar to that used for growing ZnO NWs.[13] Identifying the parameter that leads to the film formation can eventually realize a general guidance in controlling the nanostructure morphology. On the basis of additional experimental facts, a growth mechanism is proposed for explaining the morphology switch from NWs to mesoporous films (Figure 4). When a thin film (typically $<\sim$2 nm) of Au catalyst is deposited on a substrate, it can be melted into small nanodot islands (in the size range of ∼10−20 nm or smaller) at elevated temperature (>500 °C).[14] Those nanodots act as the nucleation site for ZnO crystal deposition once the vapor of ZnO is introduced into the growth chamber. This is the same initial step for both NW and film growth (Figure 4a). The ZnO nucleates typically show three groups of crystal surface: {0001}, $\{01\bar{1}0\}$, and $\{11\bar{2}0\}$, where the {0001} surfaces are perpendicular to the other two groups. The ZnO can grow along the three groups of planes but with different rates, which are controlled by the ZnO vapor concentration and kinetics. As dominated by the ionic polar charges, the {0001} surfaces require the lowest energy for ZnO deposition. As a result, moderately supersaturated ZnO vapor is adequate for the growth along the [0001] direction. Once a higher supersaturated ZnO vapor is introduced, the deposition of ZnO on the other two surfaces can be activated and accelerated with the increase in vapor pressure.

On the basis of this model, isolated aligned ZnO NWs can be achieved at a moderate ZnO vapor pressure, when only the (0001) surface deposition is activated (Figure 4b). However, the window for the formation of such a NW array is fairly small, which has been revealed in our previous research.[14] A more common outcome is the deposition simultaneously occurring along both vertical and horizontal directions at a higher ZnO vapor pressure (Figure 4c). Since the distance between nucleate sites can be as short as tens of nanometers, the horizontal grown ZnO will quickly merge together, forming a continuous network. Meanwhile, the gold catalyst dots still remain at the top of the original ZnO nucleates, catalyzing the deposition along the [0001] direction (Figure 4d). With the help of Au catalyst, ZnO can quickly deposit at the Au−ZnO junction through the vapor−liquid−solid (VLS)[15] or vapor−solid−solid (VSS)[16] process. Without the presence of any catalyst, the ZnO network between the NWs grows at a much slower rate through the vapor−solid (VS) process.[17] Thus, NWs are formed through fast growth under the Au catalyst, while a continuous network is slowly deposited, connecting the bottom of the NWs (Figure 4e). The formation of long NWs can shadow the ZnO vapor reaching the bottom network and further limited its growth rate. The SEM image shown in Figure 4e is a typical result of ZnO NWs with a bottom network catalyzed by a 2-nm Au film.

In reality, Au catalyst can be gradually consumed during the growth because of slow diffusion into the ZnO lattice.[18] If the amount of Au catalyst is so small that it can be quickly consumed at the initial growth stage, the original nucleation sites and the network between them will grow at the same slow rate through the VS process (Figure 4f), as the formation of nanobelts. Therefore, the network can be turned into continuous walls with fairly uniform heights. The small spaces between the walls are considered as pores in the ZnO wall formed film. The SEM image in Figure 4f shows a typical result of the ZnO porous film catalyzed by a 0.4-nm Au film. In addition, the slow growth rate is reflected by the 2-μm thick Au-catalyzed ZnO porous film in a 2-h deposition, while a 30-min deposition typical generates ∼3−4-μm long NWs.

The ZnO mesoporous film has been applied as a gas sensor to reveal its advantage of a significantly enlarged surface area. A sensor device was fabricated by depositing 300-nm Au electrodes on both ends of the ZnO mesoporous film. Current flowing through the ZnO film was continuously measured while

a constant DC voltage was applied between the two electrodes. The sensing property was tested in a sealed chamber, where the target gas species can be introduced at a controlled percentage. The response to CH_4 gas, as an example, is shown in Figure 5. A sharp jump of current was immediately observed once 500 ppm CH_4 in Ar gas was introduced into the testing chamber. Distinguishable conductance change was observed at 100 ppm CH_4. The mesoporous ZnO film exhibited a superior response time and changing amplitude compared to the traditional ZnO thin film solid-state gas sensors;[19,20] at the same time, it still preserves the merits of reliability and repeatability.

4. Conclusion

In summary, this paper presents a controlled, large scale fabrication of mesoporous ZnO thin films. The morphology and crystallography was carefully analyzed by electron microscopy techniques. It was revealed that the entire ZnO mesoporous film is one piece of single crystal, while a high porosity made of nanowalls is present. The growth mechanism was proposed in comparison with the growth of ZnO NWs, and a general conclusion was presented for controlling the morphology by experimental conditions, such as vapor concentration and amount of catalysts. The ZnO mesoporous film was successfully applied as a gas sensor. The fabrication and growth analysis of mesoporous ZnO thin film give general guidance in direction-controlled growth of nanostructures. Meanwhile, it also provides a unique structure with a superhigh surface-to-volume ratio for surface-related applications, such as sensing, catalyzing, energy harvesting, etc.

Acknowledgment. Research was supported by DARPA (Army/AMCOM/REDSTONE AR, W31P4Q-08-1-0009), BES DOE (DE-FG02-07ER46394), Air Force Office (FA9550-08-1-0446), KAUST Global Research Partnership, and Emory-Georgia Tech CCNE funded by NIH.

References and Notes

(1) Wang, Z. L. *Nanowires and Nanobelts, Vol. I: Metal and Semiconductor, Nanowires*; Kluwer Academic Publisher: New York, 2003.

(2) Wang, Z. L. *Nanowires and Nanobelts, Vol. II: Nanowires and Nanobelts of Functional Materials*; Kluwer Academic Publisher: New York, 2003.

(3) Pan, Z. W.; Dai, Z. R.; Wang, Z. L. *Science* **2001**, *291*, 1947.

(4) Kong, X. Y.; Ding, Y.; Yang, R.; Wang, Z. L. *Science* **2004**, *303*, 1348.

(5) Gao, P. X.; Ding, Y.; Mai, W. J.; Hughes, W. L.; Lao, C. S.; Wang, Z. L. *Science* **2005**, *309*, 1700.

(6) Wang, Z. L.; Kong, X. Y.; Zuo, J. M. *Phys. Rev. Lett.* **2003**, *91*, 185502.

(7) Wang, Z. L. *Adv. Mater.* **2003**, *15*, 432.

(8) Lao, J. Y.; Huang, J. Y.; Wang, D. Z.; Ren, Z. F.; Steeves, D.; Kimball, B.; Porter, W. *Appl. Phys. A: Mater. Sci. Process.* **2004**, *78*, 539.

(9) Ng, H. T.; Li, J.; Smith, M. K.; Nguyen, P.; Cassell, A.; Han, J.; Meyyappan, M. *Science* **2003**, *300*, 1249.

(10) Grabowska, J.; Meaney, A.; Nanda, K. K.; Mosnier, J. P.; Henry, M. O.; Duclere, J. R.; McGlynn, E. *Phys. Rev. B* **2005**, 71.

(11) JCPDS-04-003-2106, International centre for diffraction data, 2004.

(12) JCPDS-01-089-8624, International centre for diffraction data, 1999.

(13) Wang, X. D.; Song, J. H.; Li, P.; Ryou, J. H.; Dupuis, R. D.; Summers, C. J.; Wang, Z. L. *J. Am. Chem. Soc.* **2005**, *127*, 7920.

(14) Wang, X. D.; Song, J. H.; Summers, C. J.; Ryou, J. H.; Li, P.; Dupuis, R. D.; Wang, Z. L. *J. Phys. Chem. B* **2006**, *110*, 7720.

(15) Komatsu, E.; Higuchi, Y.; Niina, T. *Appl. Phys. Lett.* **1967**, *10*, 42.

(16) Kirkham, M.; Wang, X. D.; Wang, Z. L.; Snyder, R. L. *Nanotechnology* **2007**, 18.

(17) Law, M.; Goldberger, J.; Yang, P. D. *Annu. Rev. Mater. Res.* **2004**, *34*, 83.

(18) Allen, J. E.; Hemesath, E. R.; Perea, D. E.; Lensch-Falk, J. L.; Li, Z. Y.; Yin, F.; Gass, M. H.; Wang, P.; Bleloch, A. L.; Palmer, R. E.; Lauhon, L. J. *Nat. Nanotechnol.* **2008**, *3*, 168.

(19) Shinde, V. R.; Gujar, T. P.; Lokhande, C. D.; Mane, R. S.; Han, S. H. *Mater. Sci. Eng. B* **2007**, *137*, 119.

(20) Chou, S. M.; Teoh, L. G.; Lai, W. H.; Su, Y. H.; Hon, M. H. *Sensors* **2006**, *6*, 1420.

JP809358M